

# Investigation of crack propagation with different confining pressure on anisotropic gneiss

B. Vásárhelyi

Dept. of Engineering Geology, Budapest University of Technology and Economics, Budapest, Hungary

**ABSTRACT:** It is widely known that ductility increases with increasing confining pressure, and that the transition from the brittle to ductile state occurs at a certain confining pressure. This phenomena was investigated in conventional triaxial test by many researchers. The goal of this research was to examine the mechanical behavior, specially the transition from brittle to ductile behavior of anisotropic rocks with initial crack during three-point bending. Therefore the samples were performed  $0^\circ$ ,  $30^\circ$ ,  $45^\circ$ ,  $60^\circ$  and  $90^\circ$  from the horizontal foliation. The applied confining pressures were 0, 10, 30 and 60 MPa. The fracture process zone both pre- and the post-failure part can be also determined using the stress intensity factor vs. displacement and the displacement vs. crack-opening displacement curves.

## 1 INTRODUCTION

Firstly Kármán (1910, 1911), after Griggs (1936) later many other researchers (e.g. Handin & Hager 1957, Paterson 1958, Heard 1960, Orowan 1960, Byerlee 1968, Edmond & Patersen 1972, Mogi 1972, Rutter 1972, Gowd & Rummel 1980, Scott & Nielsen 1991) observed the influence of confining pressure on the behavior of rocks which were brittle at zero and low confining pressure. At high confining pressure, however, the same rocks may be ductile. That means they may fault or otherwise deform without loss of compressive strength. The amount of ductile deformation and the strength increase progressively with increasing confining pressure, until fully ductile deformation occurred with apparent work-hardening. One of the goals of this research was to examine the brittle-ductile transition of the anisotropic gneiss in case of three point bending (i.e. in case of tensile stress).

Crack propagation with high confining pressure was also examined. Crack propagation in rock is characterized by the formation of microcracks around the crack tip, and interlocking in a portion of the crack where displacements have not reached a critical value. This zone of inelastic behavior is called the fracture process zone, analogous to the plastic zone in metals (Mindess 1983). Size requirements in fracture testing need to be fulfilled to keep the length of the process zone smaller than any of the dimensions of the specimen (size, crack length, etc.).

The propagation of the crack in orthotropic gneiss was examined with the three-point bending test with different applied confining pressures (0, 10, 30 and 60 MPa). Crack propagation was investigated in five orientations with respect to the foliation of the rock ( $\ominus$ ):  $0^\circ$ ,  $30^\circ$ ,  $45^\circ$ ,  $60^\circ$  and  $90^\circ$  from the horizontal. The crack-opening displacement vs. displacement curves together with the force vs. displacement curves can be used to determine the fracture process zone.

Influence of confining pressure on three-point bending tests with prefabricated-crack was investigated by firstly Schmidt & Huddle (1977) and Abou-Sayed (1977), later Biret (1987) with isotropic rocks and by Afassi (1991) and Vásárhelyi (1995, 1997) for anisotropic rocks. According to these researches the relation between the calculated critical stress intensity factor ( $K_{Ic}$ ) and the confining pressure is linear and the slope of this line is a material constant.

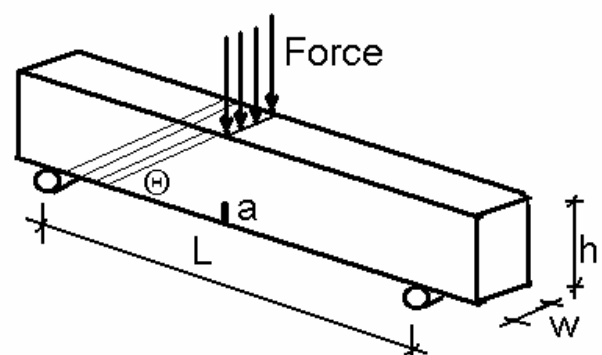


Figure 1. Dimensions of the three-point bending test specimen

The investigated anisotropic gneiss the minerals were deformed in one direction during the metamorphosis which can be seen with unaided eye. The specimen preparation, test equipment and the petrophysical constants of the rock was described by the previous papers of Vásárhelyi (1995, 1997) and Ledniczky & Vásárhelyi (2000).

Each specimen was 25 mm high ( $h$ ), 15 mm wide ( $w$ ) and the distance between the two fixed points was always 100 mm ( $L$ ). All tests were on specimens of equal size with nearly equal crack length ( $a = 5$  mm) in the middle of the bottom of the specimen (Vásárhelyi 1997). To perform tests under confining pressure, the specimens had to be jacketed under vacuum with a special, flexible material that would cover all the machined surfaces including the crack, but would not enter the crack. All specimens were air-dried and tested at room temperature.

A pressure vessel was specifically designed for confined pressure tests (see Vásárhelyi 1997). The confining pressure ( $P$ ) controlled by a servo-controlled intensifier. Light hydraulic oil was used as the pressure medium. The load was measured with a proving ring equipped with an extensometer. This instrument was located between the loading piston and the specimen. The load was increased by increasing the displacement at  $0.3 \mu\text{m/s}$ . Vertical displacement and the crack-opening displacement were measured with linear-variable differential transformers (LVDT).

## 2 BRITTLE-DUCTILE TRANSITION

At 0 MPa confining pressure the gneiss failed in a brittle way (see Fig. 2). The amount of ductile deformation and the strength increased with increasing confining pressure (10 MPa) until plastic deformation occurred (see Fig. 3) with apparent work-hardening (30, 60 MPa, see Figs. 4 and 5, respectively). It means that the brittle material became ductile with higher confining pressure not only for triaxial tests but for the tensile-bending tests (i.e. tensile stress), too.

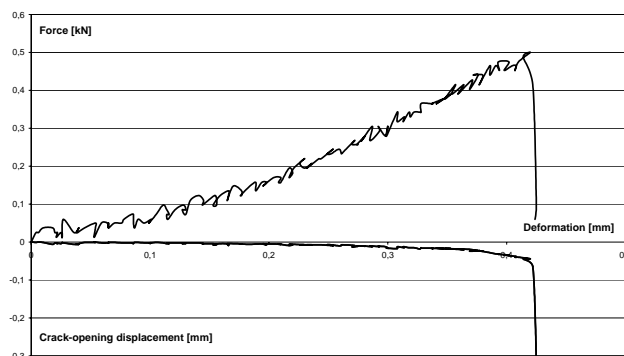


Figure 2. Crack-opening displacement vs. deformation and the force vs. deformation relation at 0 MPa confining pressure – brittle behavior.

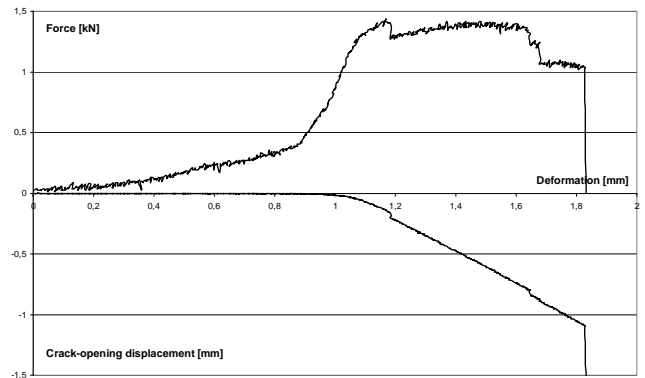


Figure 3. Crack-opening displacement vs. deformation and the force vs. deformation relation at 10 MPa confining pressure – plastic behavior.

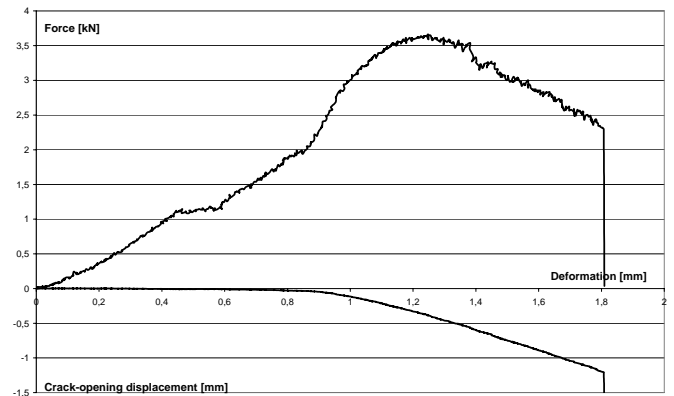


Figure 4. Crack-opening displacement vs. deformation and the force vs. deformation relation at 30 MPa confining pressure – work-hardening behavior.

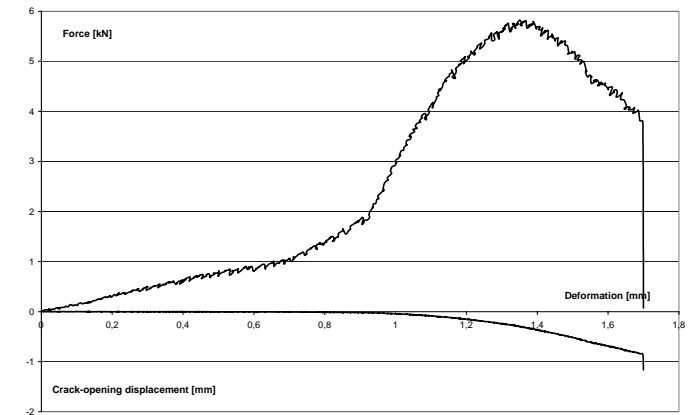


Figure 5. Crack-opening displacement vs. deformation and the force vs. deformation relation at 60 MPa confining pressure – work-hardening behavior.

Figure 6 shows the influence of the confining pressure on the force vs. deformation curve in case of the  $0^\circ$  foliation. There was no influence of the direction of the anisotropy, the results from the different directions are characteristically similar. The maximum force increases linearly with the applied confining pressure. It can be also seen that the plastic zone decrease with the increasing confining pressure while the work-hardening effect increase.

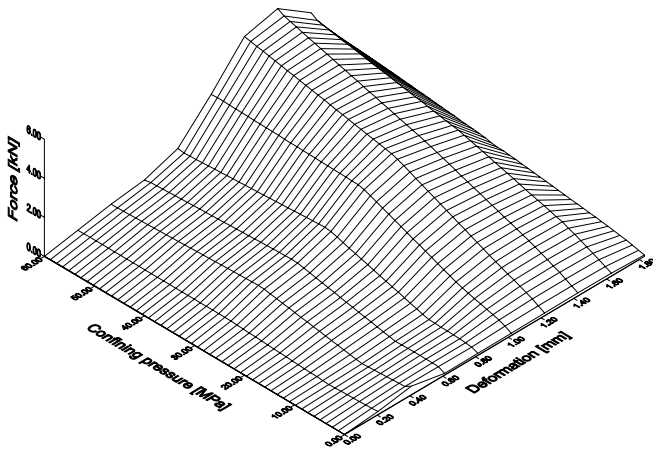


Figure 6. Three dimensional illustration of the force vs. deformation curves in function of the confining pressure. Axis: x: deformation (in mm), y: confining pressure (in MPa), z: force (in kN).

### 3 THE FRACTURE PROCESS ZONE

It is suggested that crack propagation in rocks and rock-like materials is associated with the formation of microcracks at the crack tip, and interlocking of particles behind the crack tip (also called ligament connection or crack bridging). The validity of linear-elastic fracture mechanics depends on the effects of these features on crack propagation. In rocks the region near the crack tip containing the microcracked zone and the ligament connections is called the fracture process zone (Maji & Wang 1992). The different parts of the propagating crack are shown in Figure 7.

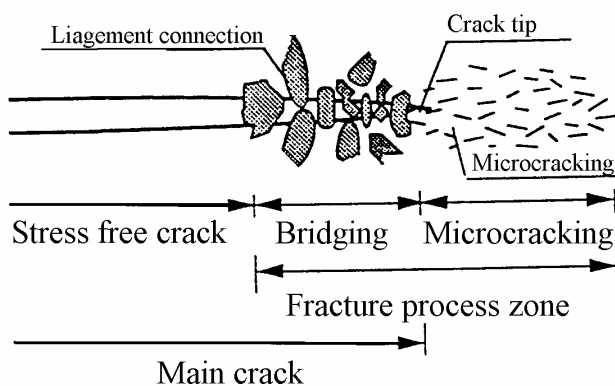


Figure 7. Theoretical model of fracture process zone (Maji & Wang 1992).

Failure of brittle rocks has been investigated by many researchers (e.g. Bieniawski 1967, Wawersik & Brace 1971, Martin & Chandler 1994). These researchers showed that the stress-strain curves for a brittle material in uniaxial compression can be divided into five regions (I: microcrack closure; II: elastic region; III: stable crack growth; IV: unstable crack growth and V: failure). For three-point

bending, except for 0 MPa confining pressure, the force vs. displacement curve using the crack-opening displacement vs. displacement curve can be divided into three parts followed by failure. Figure 8 illustrates these four regions.

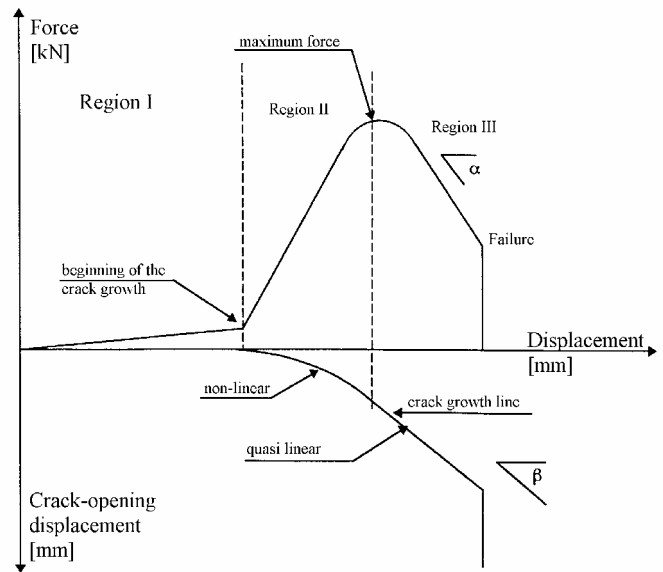


Figure 8. Schematic illustration of the force vs. deformation and crack-opening displacement vs. deformation curves

**Region I:** There is no crack-opening displacement, only displacement in the vertical direction. In this part, the micro-cracks were formed. The force-displacement curve is linear.

**Region II:** The beginning of the crack growth. In this region the crack-opening displacement is not zero and the relation between the crack-opening displacement and deformation is non-linear. The end of this region is at the maximum force. The force-displacement curves consist of some linear parts but near the fracture toughness they become non-linear. The slope of the force-displacement curves increases with the higher confining pressure.

**Maximum force:** The fracture toughness can be calculated at this point. It depends on linearly with the applied confining pressure (Ledniczky & Vásárhelyi 2000).

**Region III:** This is the post-critical part of the force-deformation curve. The force decreases linearly and this linear curve is different for the three different confining pressures. The material is plastic at 10 MPa hydrostatic pressure. At higher applied pressure, the post-critical range becomes longer and longer and the force decrease slope ( $\alpha$ ) becomes steeper. The relation between the slope of the post-critical part ( $\tan \alpha$ ) and the confining pressure ( $P$ ) is linear:

$$\tan(\alpha) = aP - b$$

Analyzing the curves the results show that there is practically no difference between the different directions: the value of  $a$  and  $b$  is around 0.13 and 1.38, respectively.

The crack-opening displacement vs. deformation curve ( $\beta$ ) can be approximated by a straight line from the beginning of the maximum force to failure. For 0 MPa this angle was not determinable. As the results show, the slope of this curve increases with confining pressure, but the relation between the two ( $\beta$  and  $P$ ) could not be written exactly.

Region IV: Failure.

#### 4 CONCLUSION

Forty three-point bending tests were carried out on an anisotropic gneiss in five directions of the foliation (0°; 30°; 45°; 60° and 90°) and under four differences hydrostatic pressures (0; 10; 30 and 60 MPa). There was no significant difference between the results for samples deformed in the different directions. The brittle rock became ductile and work-hardening at higher confining pressure. The changing of these behavior was shown with three dimensional figure.

Crack growth and the development of fracture process zone under different confining pressures was also investigated. The fracture process zone was determined by using the force vs. deformation and crack-opening displacement vs. displacement curves. Using these curves the fracture process can be divided into three parts followed by failure in case of three point bending tests (i.e.: microcracks initiation, coalescence of the microcracks and the crack growth).

Also there is a linear relation between the tangent of the slope of the curve in post-critical region and confining pressure.

Using these results it is possible to define the material constants which are necessary for the exact thermodynamical equations of the crack propagation (Ván 2001, Ván & Vásárhelyi 2001).

#### 5 ACKNOWLEDGEMENT

The author thanks for Mme. F. Homand-Etienne, professor of the INPL-Nancy for her advice and for the French Government supporting this research with BGF scholarship at Nancy, France.

#### 6 REFERENCES

Abou-Sayed, A.S. 1977. Fracture toughness  $K_{IC}$  of triaxially loaded Indiana limestone. *Proc. 17<sup>th</sup> Symp. Rock Mech. (Keystones)*, 2 A3-1–2 A3-8.

Afassi, F. 1991. *Caractérisation de la résistance à la propagation des fissures dans une roche anisotrope: le schiste*. These de Doctorat, Univ des Sci. et Techn. de Lille.

Bieniawski, Z.T. 1967. Mechanism of brittle fracture of rock, *Int. J. Rock. Mech. Min. Sci. & Geomech. Abstr.* **4**:395-430.

Biret, F. 1987. *Mesure de l'influence de la pression sur la propagation de fissure dans les roches*. These de Doctorat, Université de Bordeaux I.

Byerlee, J.D. 1968. Brittle-ductile transition in rock. *J. Geophys. Res.* **73**(14): 4741-4750.

Edmond, J.M. & Paterson, M.S. 1972. Volume changes during the deformation of rocks at high pressures, *Int. J. Rock Mech. Min. Sci.* **9**: 161-182.

Gowd, T.N. & Rummel, F. 1980. Effect of confining pressure on the fracture behavior of a porous rock. *Int. J. Rock Mech. Min. Sci.* **17**: 225-229.

Griggs, D.T. 1936. Deformation of rocks under high confining pressures. *J. Geol.* **44**: 541-577.

Handin, J. & Hager, R.V. 1957. Experimental deformation of sedimentary rocks under confining pressure: tests at room temperature on dry samples, *Bull. Am. Assoc. Petrol. Geologist*, **41**(1): 1-50.

Heard, H.C. 1960. Transition from brittle fracture to ductile flow in Solenhofen limestone as a function of temperature, confining pressure, and interstitial fluid pressure, *Rock Deformation, Geol. Soc. Am.* **79**: 193-226.

Kármán, T. 1910. Mitől függ az anyag igénybevétele? *Magyar Mérnök és Építészegylet Közlönye*, **10**: 212-226 .

von Kármán, T. 1911. Festigkeits Versuche unter allseitigem Druck, *Verhandl. Deut. Ingr.* **55**: 1749-1757.

Ledniczky, K. & Vásárhelyi B. 2000. Brittle-ductile transition of anisotropic rocks during three-point bending tests. *Acta Geod. Geoph. Hung.* **35**(1): 75-80.

Maji, A.K. & Wang, J.L. 1992. Experimental study of fracture process in rock. *Rock Mech. Rock Engng.* **25**(1): 25-47.

Martin, C.D. & Chandler, N.A. 1994. The progressive fracture of Lac du Bonnet granite, *Int. J. Rock. Mech. Min. Sci. & Geomech. Abstr.* **31**: 643-659.

Mindess, S. 1983. The application of fracture mechanics to cement and concrete: a historical review. In F.H. Wittmann, (ed.) *Fracture Mechanics of Concrete*: 1-41 Amsterdam: Elsevier.

Mogi, K. 1972. Fracture and flow of rocks, *Tectonophysics* **21**: 273-285.

Orowan, E. 1960. Mechanism of seismic faulting, *Rock Deformation, Geol. Soc. Am.* **79**: 325-345.

Paterson, M.S. 1958. Experimental deformation and faulting in Wombeyan marble, *Bull. Geol. Soc. Am.* **69**: 465-476.

Rutter, R.H. 1972. The effect of strain-rate changes on the strength and ductility of Solenhofen limestone at low temperatures and confining pressures. *Int. J. Rock Mech. Min. Sci.* **9**: 183-189.

Schmidt, R.A. & Huddle, C.W. 1977. Effect of confining pressure on fracture toughness of Indiana limestone. *Int. J. Rock Mech. Min. Sci. & Geomech. Abstr.* **14**: 289-293.

Schmidt, R.A. 1980. A microcrack model and its significant to hydraulic fracturing and fracture toughness testing. *Proc. 21<sup>st</sup> U.S. Symp. on Rock Mech.* 581-590.

Scott, Th.E. & Nielsen, K.C. 1991. The effects of porosity on the brittle-ductile transition in sandstones. *J. Geophys. Res.* **96**(B1): 405-414.

Ván, P. 2001. Internal thermodynamic variables and failure of microcracked materials. *J. Noneq. Thermodyn.* (in submission).

Ván, P. & Vásárhelyi, B. 2001. Second Law of thermodynamics and failure of rock materials. *38<sup>th</sup> US Rock Mech. Symp., DC Rocks*, Washington D.C. (in print).

Vásárhelyi, B. 1995. *Etude de l'influence de la pression de confinement et de l'orientation de la foliation sur la propagation des fissures dans un gneiss*, Rapport de Stage, INPL-Nancy.

Vásárhelyi, B. 1997. Influence of pressure on the crack propagation under mode I loading in anisotropic gneiss. *Rock Mech. Rock Engng.* **30**(1): 59-64.

Wawersik, W.R. & Brace, W.F. 1971. Post failure behaviour of a granite and diabase. *Rock Mech. Rock Engng.* **3**(2): 61-85.